



ASSESSMENT OF THE COLLAPSE RISK OF INFILL WALLED BUILDINGS

V.H. Akansel⁽¹⁾, J. P. Moehle⁽²⁾

⁽¹⁾ Middle East Technical University (on leave from Muğla Sıtkı Koçman University), Research Assistant, akansel@metu.edu.tr

⁽²⁾ University of California, Berkeley, Professor, moehle@berkeley.edu

Abstract

Infill walls in reinforced concrete buildings can strongly affect the strength and deformation capacity of the building when subjected to earthquake loading. Global effects include overall stiffening and strengthening of stories containing infills. Where infills fail by in-plane or out-of-plane loading, soft/weak stories can occur, leading to concentrated story drift demands. Infills can also affect structural members on a local level. Such effects include increased axial forces on columns due to overturning, concentrated shear forces at the ends of beams and columns, and localized deformations in columns surrounded by discontinuous infills. Such effects should be considered when assessing or rehabilitating an older existing concrete building with infills.

In this study, we are primarily concerned with the effect of infill walls on the collapse risk of older existing concrete buildings. Analytical models are assembled in which the infill walls are modelled with macro modelling approaches. Results will be compared with the experimental results for validation of the modelling approach and then frames designed based on ACI 318 will be studied with infill walls to investigate how the story drifts and story strengths change compared to the bare frames. Effects on collapse risk will be assessed within the framework of the ongoing ATC 78 project.

Keywords: Vertical irregularity, infill wall, MRF, RC



1. Introduction

Rehabilitation of old buildings is a fundamental part of seismic risk mitigation. Among older buildings, reinforced concrete frames, including frames with infills, are recognized as posing a particularly high risk in many seismic regions of the world. Ongoing work (Galanis, 2014, and others) is developing methods to establish the collapse risk of bare frames. The present study aims to extend that work to include reinforced concrete frames with infill walls. Observations in many past earthquakes, as well as recent research (Hashemi and Mosalam, 2006; Das and Nau, 2003) demonstrate that infill walls can have significant effect on the strength capacity, drift capacity, and local failure mechanisms of a building. Therefore, such effects should be considered in the assessment of infilled frames.

Several past studies have provided a basis for the current study. Mehrabi et al. (1996) tested infilled RC frames under monotonic and reversed cyclic lateral loads. They investigated the failure mechanism of the infill walls and gave a damage index for failure mechanisms. Crisafulli et al. (1997) studied analytical modelling of the infilled frames and compared the results with experiments. They studied the similarities and differences of various infill wall models reported in the literature. Dolsek and Fajfar (2002) developed an analytical model for infilled reinforced concrete frames based on dynamic test results. They stated in their research that the most uncertain part in their model is the contact region between the infill and the reinforced concrete frame. The authors also emphasized that the results may change dramatically even for a previously damaged frame and it is thought hard to estimate. El-Dakhkhni et al. (2003) developed a three strut model, which represents the failure mechanism for infilled steel frames. The proposed model gives opportunity to make nonlinear analysis of the infill walls. This three strut model is based on the contact region between the infill wall and the frame. Öztürk (2005) studied performance of infilled frames based on FEMA 273 and Smith and Carter's methods. Only linear assessment was considered in his study. Shing P. vd. (2009) studied performance of infilled RC frames in shaking table experiments and quasi-static tests. They used micro modelling with finite element methodology to model the experimental results. Fenerci (2013), Redmond et al. (2015) and Ezzatfar et al. (2014) studied pseudo-dynamic experimental set-up with micro and macro modeling approaches and made assessment based on the criteria of ASCE 41.

2. Modeling and Verification

OpenSees (2015) software was used for the modeling. Force-based element type; nonlinear-beam-column element was used for the column and beams with fiber section definitions. Concrete02, linear tension softening material model was used. Confined material properties are calculated according to the modified Kent and Park material model. Steel02 material, Giuffrè-Menegotto-Pinto model with isotropic strain hardening was used for rebar material model. Concrete07 was used for the infill wall material and only compression was modelled (Fig. 1). For infills, three strut models are preferred for the further study of the short column effects (Fig. 2). ASCE41 modelling parameters were selected (Eq. (4-6)).

$$a = 0.175 \cdot (\lambda_1 \cdot h_{col})^{-0.4} \cdot r_{inf} \quad (4)$$

$$\lambda_1 = \left[\frac{E_{inf} \cdot t_{inf} \cdot \sin(2\theta)}{4 \cdot E_{fr} \cdot l_{col} \cdot h_{inf}} \right]^{1/4} \quad (5)$$

$$z = \frac{\pi}{2 \cdot \lambda_1} \quad (6)$$

where;

h_{col} : Column height between centerlines of beam

h_{inf} : Height of infill panel

E_{fr} : Expected modulus of elasticity of frame material

E_{inf} : Expected modulus of elasticity of infill materials

I_{col} : Moment of inertia of column

r_{inf} : Diagonal length of infill panel

t_{inf} : Thickness of infill panel and equivalent strut

θ : Angle whose tangent is the infill height-to-length aspect ratio, in radians.

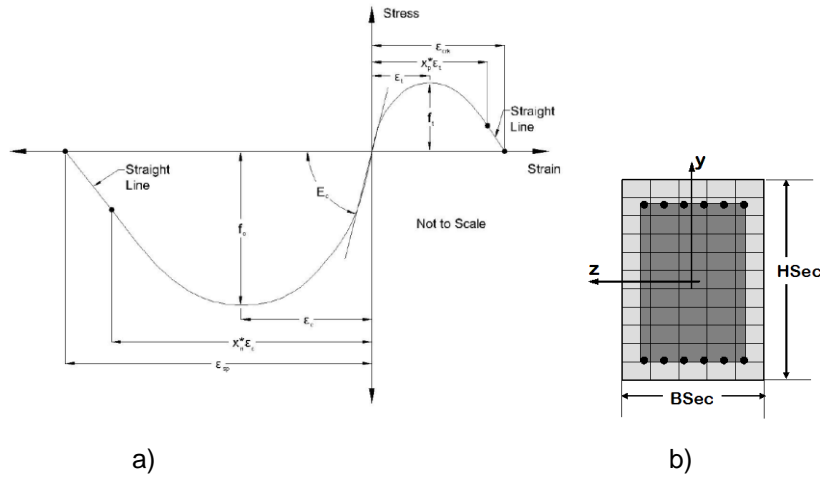


Fig. 1 – a) Concrete07 Material Model for Infill Walls; b) Fiber section definition

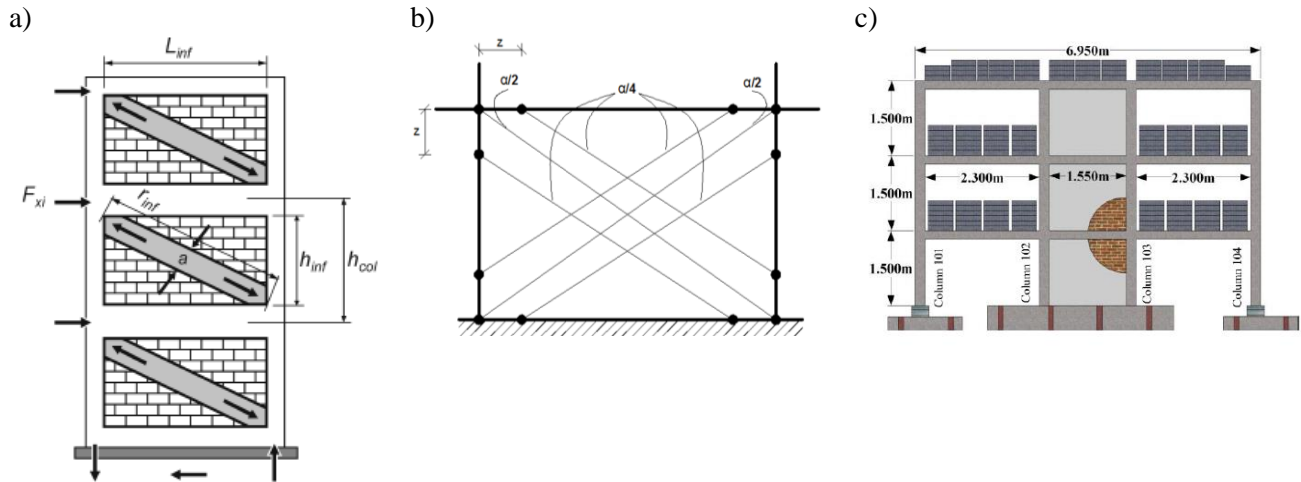


Fig. 2 – a) ASCE41 Concentric compression strut model b) three strut model c) METU Specimen (Fenerci 2013)
 Infill wall parameters are defined according to the given formulas in Eq. (7).

$$f_s = \frac{f_m t}{1.5(f_m + f_t)} \quad G = \frac{E}{2(1+\theta)} \quad f_t = \frac{f_m}{10} \quad f_m > 5 \quad k = \frac{E w_e t}{2(1+\theta)h}$$

$$N_y = \frac{f_s t d}{1000} \quad \Delta_y = \frac{N_y}{k}$$

(7)

Contact length in the models was taken as $z/3$ based on literature and experimental results and the sensitivity analysis results. Compression strength of the infill, f_c' , is calculated based on the infilled walls axial load capacity calculated from the shear diagonal failure mechanism. Yielding strain has been chosen as 0.003 based on the experimental results from the Mehrabi et al. (1996), Bal et al. (2008), Fenerci (2013), Redmond et al. (2015), and Ezzatfar et al. (2014).

Results of the analytical model were compared with various experimental results. Tests were done for one bay frame with infill walls reported by Mehrabi et al (1998) for comparison. Another 3 story, 3 bay frame experiment from Fenerci (2013) was also studied. The details of the experiments are in the related papers. The results of the verification and validation study is given in Fig. 3- 4. Contact length, z , was taken half of what it is in the Fig 3-4.

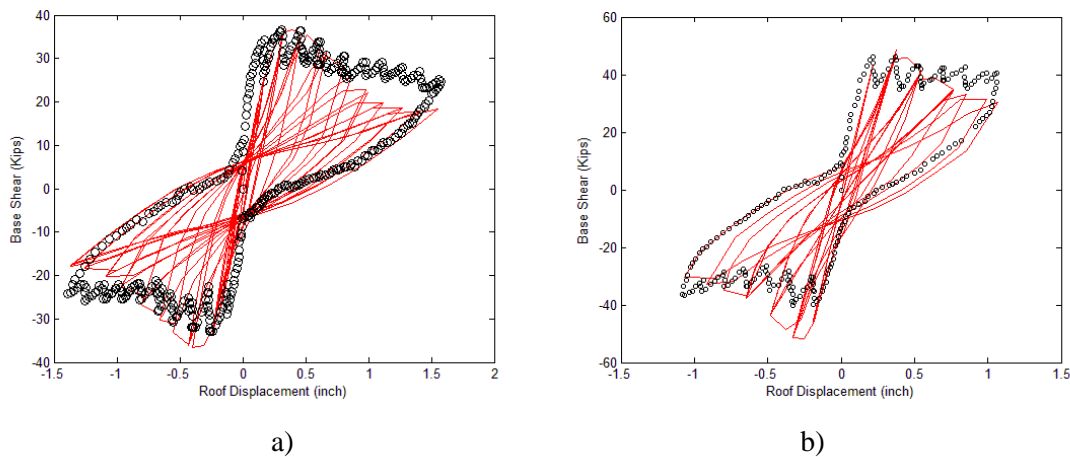


Fig. 3 – a) Specimen 4 Weak Frame - Weak Infill Cyclic Three Strut Model; b) Specimen 6, Strong Frame - Weak Infill, Three Strut Model (Mehrabi (1996)) – Red line numerical results and the black marks are envelope of cyclic experimental results

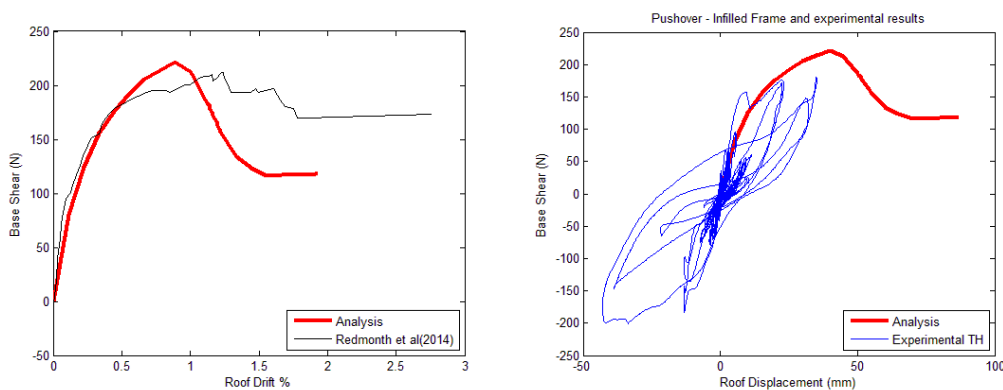


Fig. 4 – Metu Test Specimen, (a) Comparison with Redmond et.al. (2015); (b) Comparison with Experimental Study (Ezzatfar (2014))

In Fig. 4, the Metu test specimen was studied by Fenerci (2013), Ezzatfar et al. (2014) and Redmond (2015). In this test structure, there are infill walls in the mid bay (Fig 2c). Ezzatfar et al. (2014) made the experimental studies and Fenerci (2013) and Redmond et al. (2015) developed numerical models for verification.



Redmond et. al. (2015) results are used for comparison. They used contact elements for interaction of the brick to mortar and infill wall to reinforced concrete frame.

2.1 Sensitivity Analysis

Sensitivity analysis was made to see how the infill wall parameters affect the results. Sensitivity analysis were done for the three-story, three-bay METU test specimen with the middle bay infilled, which was studied by Fenerci (2013), Redmond et.al. (2015), and Ezzatfar et.al. (2014). This frame was chosen as being more realistic than one-bay experiments. Table 1 shows the various sensitivity study cases. In the first 4 cases, compressive strength of the infill wall was varied. In Cases 5 through 8, the Young modulus of the infill masonry was varied. In Cases 9 through 12, the contact length was varied. In Cases 13 through 16, the yield strain of the infill material was varied. Finally, for the last four cases, the ductility parameter for the material model Concrete07 was varied.

Table 1 – Sensitivity Study Cases

CASE	$f_t (*f_m)$	$E_m (*f_m)$	z	ϵ_m	X_n
1	0.09	750	$z/2$	0.003	2
2	0.07	750	$z/2$	0.003	2
3	0.05	750	$z/2$	0.003	2
4	0.03	750	$z/2$	0.003	2
5	0.09	550	$z/2$	0.003	2
6	0.07	550	$z/2$	0.003	2
7	0.05	550	$z/2$	0.003	2
8	0.03	550	$z/2$	0.003	2
9	0.09	550	$z/3$	0.003	2
10	0.07	550	$z/3$	0.003	2
11	0.05	550	$z/3$	0.003	2
12	0.03	550	$z/3$	0.003	2
13	0.09	550	$z/3$	0.0015	2
14	0.07	550	$z/3$	0.0015	2
15	0.05	550	$z/3$	0.0015	2
16	0.03	550	$z/3$	0.0015	2
17	0.09	550	$z/3$	0.0015	4
18	0.07	550	$z/3$	0.0015	4
19	0.05	550	$z/3$	0.0015	4
20	0.03	550	$z/3$	0.0015	4

The results of the sensitivity analysis are given in Table 2. In Table 2, “* f_m ” means that the parameter is chosen a coefficient times f_m . For example, f_t was chosen $0.07*f_m$. In Fig. 5, the sensitivity analysis results are displayed. Yield strain seems effective at increasing the initial stiffness, however, decreasing the yield strain results in meaningless failure mechanisms. For this reason, the variable was kept 0.003, which is consistent with findings of Mehrabi et al. (1996) and Bal et al. (2008). In Fig. 6, the pushover curves for the Table 2 parameters are compared with the Redmond et al. (2015) curves. Based on sensitivity analysis, tensile strength of infill wall, young modulus, contact length and yield strain of infill material model were selected as given values in Table 2.

Table 2 – Sensitivity Analysis Results

CASE	f_t ($*f_m$)	E_m ($*f_m$)	z	ϵ_m	X_n
Decided	0.07	550	$z/3$	0.003	2

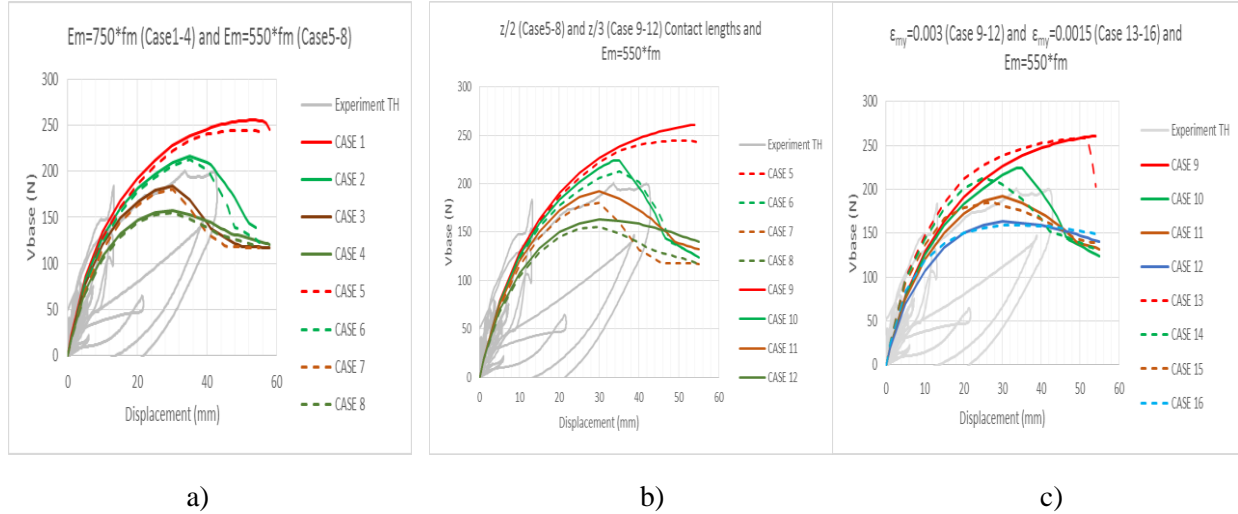


Fig. 5 – a) Youngs Modulus Comparison, b) Contact Length Comparison, c) Yield Strain of Infill Material Comparison

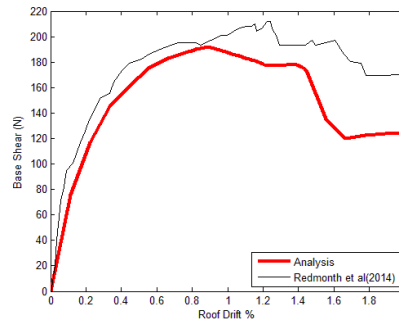


Fig. 6 – Metu Test Specimen $z=z/3$, Comparison with Redmond et.al. (2015)

3. Model Building Frames

Three RC infilled frames from Galanis (2014) (Fig. 7) were modelled in OPENSEES with same element and material types as explained previously. The detailed information on the frame designs can be found in Galanis (2014). Modeled frames are designed with $V_p/V_n=0.6$ (such that ductile flexural response is expected) and $\sum M_{nc}/\sum M_{nb}=1.2$ at beam-column joints. Interior frames were selected. Compressive strength of the infill wall was taken as 1 ksi and thickness of the infill was taken as 6 in. Compressive strength of concrete is 3 ksi and yield strength of the steel was taken as 60 ksi. The compressive strength of the infill wall was taken as 1 ksi. Young Modulus of the infill masonry was taken as $550*f_m$. Concrete compressive strength is 3 ksi and young modulus was calculated from the ACI318. Same modelling methodology was preferred for the frames. Some parameters of interest include: α =Story Drift Ratio/ Drift Ratio at Effective modal height (Modal height is considered as $0.7h$ for the calculations); Strength Ratio and DCR (Demand to Capacity Ratio).

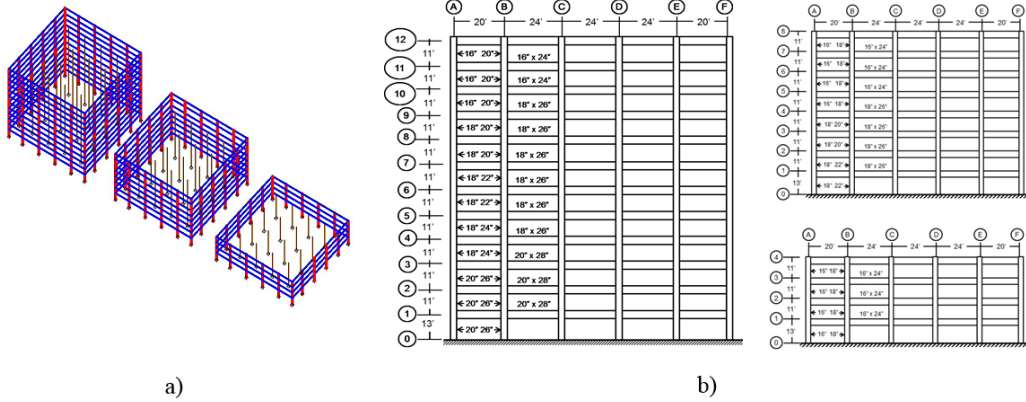


Fig. 7 – Galanis (2014) Frames, a) 3D view, b) 12, 8 and 4 story frames

A matlab script was written to post-process the analysis results to investigate various parameters. M_{pr} was calculated for the section analysis calculated according to ACI 318. Steel01 was used for M_{pr} calculation. Matlab script calculates yield curvature from section analysis and reads the results of the pushover analysis for each member ends and takes ratios of this values (Pushover result/Section analysis yield curvature result). Script puts a mark if the curvature ratio is greater than one.

4. Analysis and Results

4.1 Nonlinear Pushover Analysis

Inverted triangular load pattern was applied for pushover analysis to bare and infilled frames. Figure 8 plots typical results for a 12-story tall bare frame deformed to roof drift ratio = 0.02. Normalized base shear coefficient is around 0.11 and maximum shear demand to capacity ratio (DCR) is 1.2. Due to limitation of pages, only 12 story failure mechanisms are given in Fig.8 and Fig.9. Mean strength ratio for 8 story building bare frame is 1.52. Normalized base shear for 8 story bare frame is 0.25 and maximum demand to capacity ratio is 1.0. Corresponding values for 4 story building is accordingly 1.202, 0.16 and 1.0.

Table 3 –Ratio of maximum normalized base shear of infilled frames to bare frame

Story	(Infilled)/Bare	(Infilled w/o 1 st)/Bare	(Infilled w/o 2 nd)/Bare	(Infilled w/o mid bay 2,4)/Bare
4 Story	3.76	1.07	1.53	2.54
8 Story	2.77	1.28	1.71	1.97
12 Story	2.25	1.63	1.59	1.7

Figures 9, 10 and 11 present failure mechanisms, pushover curves, and α values of frames with different infill wall layouts at roof drift ratios of 0.01 and 0.02. The presence and layout of the infill masonry strongly affects the failure mechanism of the system. α parameter seems to be a good identifier for vertical irregularities, especially for soft or weak story mechanisms.

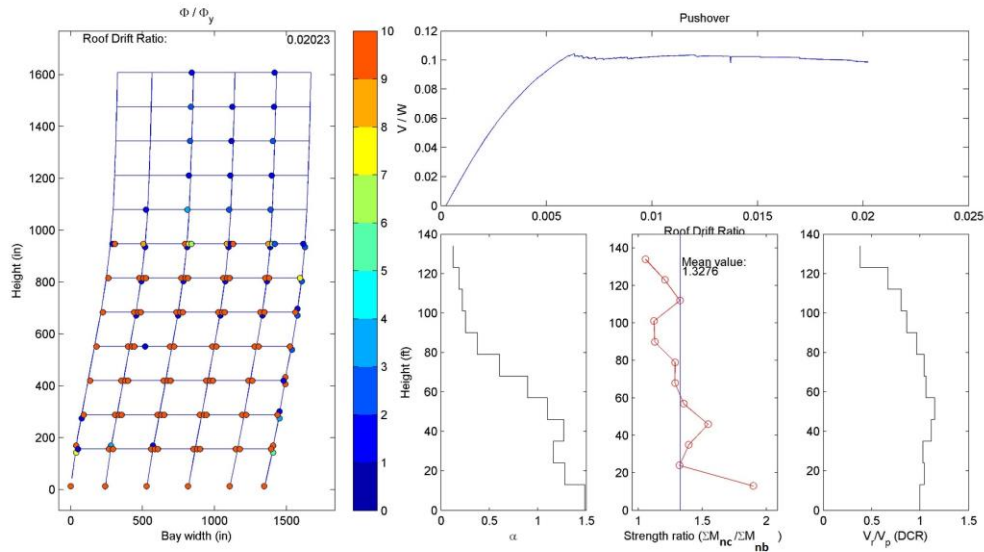


Fig. 8 – 12 Story Bare Frame.

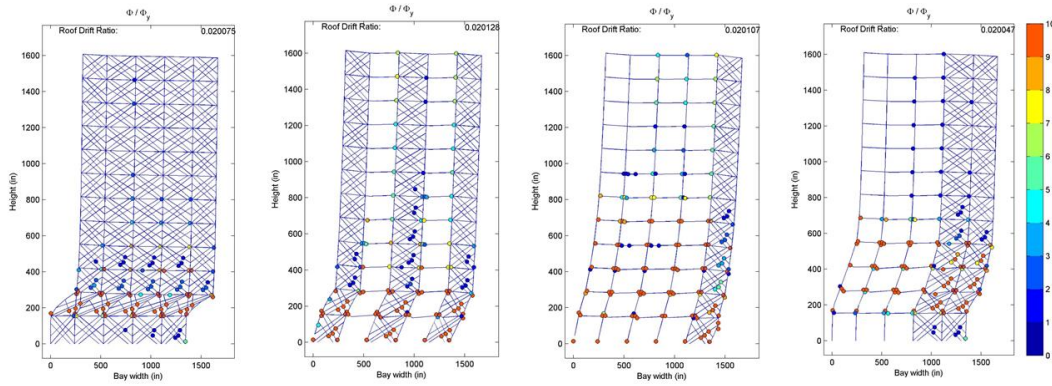


Fig. 9 – 12 Story Frame Failure Mechanism at 0.02 roof drift ratio for different infill wall arrangements

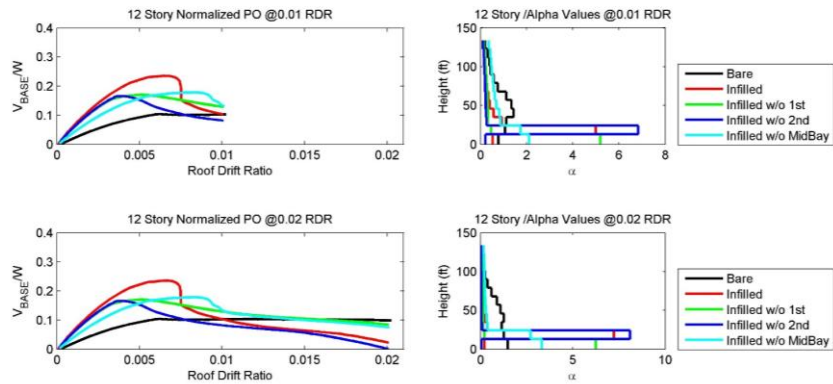


Fig. 10 – 12 Story Results Summary

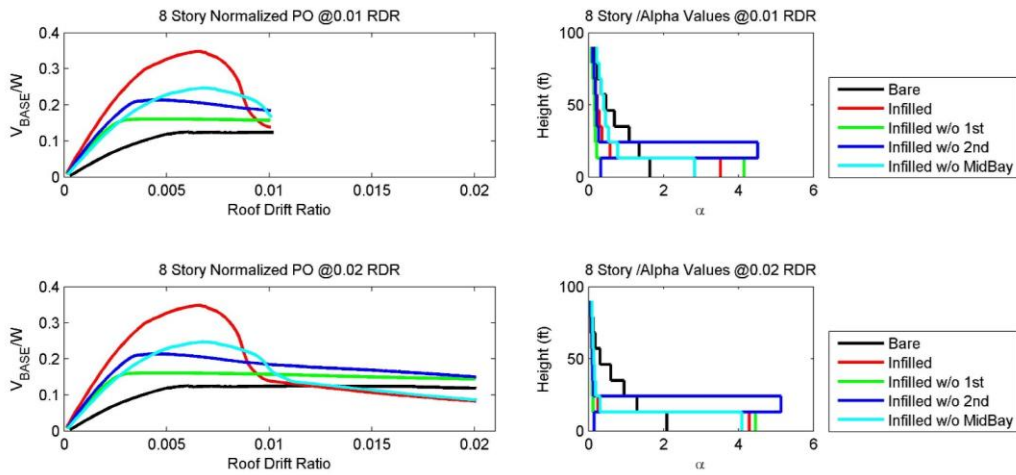


Fig. 11 – 8 Story Results Summary

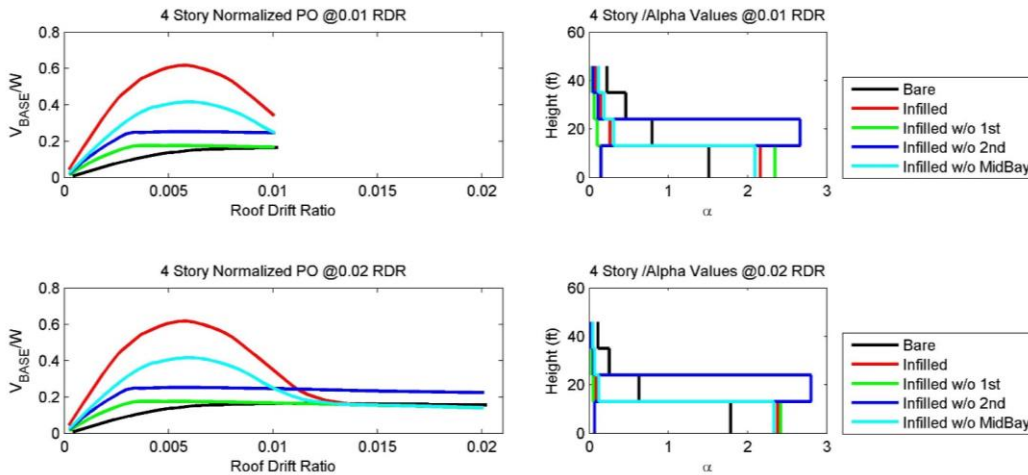


Fig. 12 – 4 Story Results Summary

4.2 Dynamic Analysis

A set of 20 earthquake ground motions was selected and scaled using the method provided by Baker and Cornell (2006) and Baker (2011). First a seismic hazard analysis was done using the USGS website Earthquake Hazard Program. UC, Berkeley is selected as the building site. Soil type was assigned as Type D. In Table 4, the calculated spectral acceleration values are given. In Fig. 13, Modal (R , M , ϵ_0) from peak R , M bin was considered for the ground motion selection. Unconditional but scaled selection was done (Fig. 13b and 13c). Ground motions were selected and scaled to match the target spectrum for a period range including natural period and 1.5 times of natural period. This method is conservative but adequate for the intended results. PEER NGA-WEST2 database was used for the selection of the ground motions. Table 5 lists the selected ground motions.

Table 4 – Spectral Acceleration values for site specific spectrum

S_s	S_1	S_{MS}	S_{M1}	S_{DS}	S_{D1}
2.199 g	0.849 g	2.639 g	1.443 g	1.759 g	0.962 g

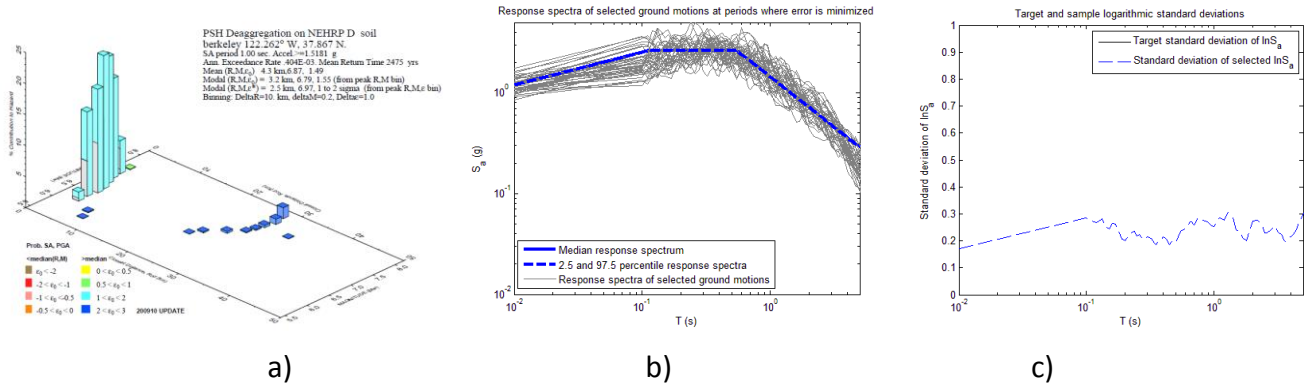


Fig. 13 – a) PSH Deaggregation on NHRP D Soil for UC, Berkeley, b) Selected ground motions for the maximum considered earthquake and standard deviation of ground motion set.

Table 5 – Selected ground motions

Record Number	NGA Record Sequence Number	Scale Factor	Dir. 1	Dir. 2
1	169	3.9	IMPVALL/H-DLT262.at2	IMPVALL/H-DLT352.at2
2	126	2.2	GAZLI/GAZ000.at2	GAZLI/GAZ090.at2
3	1511	3.2	CHICHI/TCU076-E.at2	CHICHI/TCU076-N.at2
4	183	3.1	IMPVALL/H-E08140.at2	IMPVALL/H-E08230.at2
5	779	2	LOMAP/LGP000.at2	LOMAP/LGP090.at2
6	179	3.2	IMPVALL/H-E04140.at2	IMPVALL/H-E04230.at2
7	184	3	IMPVALL/H-EDA270.at2	IMPVALL/H-EDA360.at2
8	802	3.7	LOMAP/STG000.at2	LOMAP/STG090.at2
9	1013	3.1	NORTHR/LDM064.at2	NORTHR/LDM334.at2
10	721	4	SUPERST/B-ICC000.at2	SUPERST/B-ICC090.at2
11	1489	4	CHICHI/TCU049-E.at2	CHICHI/TCU049-N.at2
12	1085	2.1	NORTHR/SCE018.at2	NORTHR/SCE288.at2
13	1158	3.2	KOCAELI/DZC180.at2	KOCAELI/DZC270.at2
14	1495	4	CHICHI/TCU055-E.at2	CHICHI/TCU055-N.at2
15	803	3.7	LOMAP/WVC000.at2	LOMAP/WVC270.at2
16	1546	4	CHICHI/TCU122-E.at2	CHICHI/TCU122-N.at2
17	1521	4	CHICHI/TCU089-E.at2	CHICHI/TCU089-N.at2
18	292	3.6	ITALY/A-STU000.at2	ITALY/A-STU270.at2
19	180	2.5	IMPVALL/H-E05140.at2	IMPVALL/H-E05230.at2
20	821	2.5	ERZIKAN/ERZ-NS.at2	ERZIKAN/ERZ-EW.at2

Dynamic analysis was performed for a frame having infills in each bay and the results are plotted at 0.02 story drift ratio which is thought that close to collapse limit. In Fig. 14, the mean of α values yields to 1 for this one case, however there is a huge variance. Average α parameter yields around 1.0 for nonlinear response history analysis results. This is compatible with the ATC 78 for bare frames. However, the results are done only one type of infill wall arrangement and to be able to make a generalization for α parameter, more response history analysis should be done. The study will be extended for other infill wall arrangements for dynamic analysis.

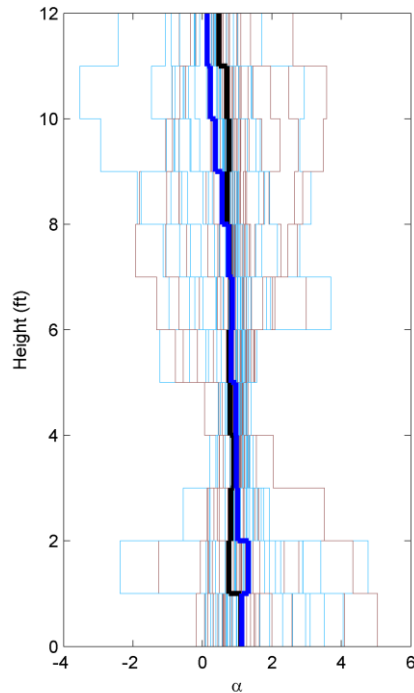


Fig. 14 – Infilled at each bay for 12 Story Frame at SDR (story drift ratio) = 0.02

5. Conclusions

Three strut models for infill walls were implemented to study the effect on static and dynamic response of multi-story frames. It is observed that the infill walls strongly affect the failure mechanism and should be considered in calculations. The parameter α provides a good identifier of soft/weak stories. The study will be extended for other infill wall arrangements for dynamic analysis.

6. Acknowledgements

This research was supported by TUBITAK 2214 –A Scholarship for International Research during PhD Program. First author also thanks her colleagues; Pablo Parra, Carlos Arteta, and Selim Günay from UC, Berkeley who provided insight that greatly assisted the research.

7. References

- [1] Shahrooz M., and Moehle J. P. (1990(b)): Evaluation of Seismic Performance of Reinforced Concrete Frames. *Journal of Structural Engineering*, vol. **116**, No. 5.
- [2] Seneviratna G.D.P.K. and Krawinkler H. (1997): Evaluation of Inelastic MDOF Effects for Seismic Design. *The John A. Blume Earthquake Engineering Center, Stanford University, Report No: 120*.
- [3] Shome N., Cornell A., Bazzurro P., and Carballo E. (1998): Earthquakes, Records, and Nonlinear Responses: *Earthquake Spectra*, Vol. 14, No. 3.
- [4] Das S. and Nau J. M. (2003): Seismic Design Aspects of Vertically Irregular Reinforced Concrete Buildings. *Earthquake Spectra*, vol. **19**, No. 3.



- [5] Soni D. P. and Mistry B. B. (2006): Qualitative Review of seismic Response of Vertically Irregular Building Frames”. *ISET Journal of Earthquake Technology*, Technical Note, Vol. 43, No. 4.
- [6] Sucuoglu, H. and Erberik, A. (1997): Performance Evaluation of a Three-Storey Unreinforced Masonry Building During the 1992 Erzincan Earthquake. *Earthquake Engineering and Structural Dynamics*, Vol. 26, pp. 319-336.
- [7] Smith, B.S. and Carter, C. (1969): A Method of Analysis for Infilled Frames. *Proc. ICE*, Vol. 44, pp.31-48, September.
- [8] Crisafulli, F.J. (1997): Seismic behavior of reinforced concrete structures with masonry infills. *University of Canterbury*, Ph.D. Thesis, Christchurch, New Zealand.
- [9] Crisafulli, F.J., Carr, A.J. and Park, R. (2005): Experimental response of framed masonry structures designed with new reinforcing detail. *Bulletin of the New Zealand Society for Earthquake Engineering*, Vol. 38, No. 1, pp 19-32.
- [10] Mehrabi, A.B., Benson Shing, P., Shculler, M.P. and Noland, J.L. (1996): Experimental evaluation of masonry-infilled RC frames. *J. Struct. Eng.*, ASCE, 122(3), 228-237.
- [11] Redmond L., Ezzatfar P., DesRoches R., Stavridis A, Özcebe G. and Kurç Ö. (2015) ; Finite Element Modeling of a Reinforced Concrete Frame with Masonry Infill and Mesh Reinforced Mortar Subjected to Earthquake Loading. *Earthquake Spectra*, Vol. 32, No. 1, pp. 393-414
- [12] Ezzatfar, P., Binici, B., Kurc, O., Canbay, E., Sucuoglu, H., and Ozcebe, G., (2014): Application of mesh reinforced mortar for performance enhancement of hollow clay tile infill walls. *Seismic Evaluation and Rehabilitation of Structures*, Vol 26, Springer International Publishing, Switzerland, 171-186
- [13] OpenSees (2015), V.2.4.6., Pacific Earthquake Engineering Research Center, UC, Berkeley.
- [14] Hashemi A. and Mosalam K. (2007): Seismic Evaluation of Reinforced Concrete Buildings Including Effects of Masonry Infill Walls. *Pacific Earthquake Engineering Research Center*, UC, Berkeley.
- [15] Bal I.E., Crowley H., and Pinho R., (2008): Displacement-Based Earthquake Loss Assessment for an Earthquake Scenario in Istanbul. *Journal of Earthquake Engineering*, 12:S2, 12-22, DOI: 10.1080/13632460802013388
- [16] Galanis P. (2014): Probabilistic Methods to Identify Seismically Hazardous Older-Type Concrete Frame Buildings. *UC, Berkeley*, PhD Thesis.
- [17] Baker J. W. and Cornell C. A. (2006): Spectral Shape, Epsilon and Record Selection. *Earthquake Engineering and Structural Dynamics*. 35:1077-1095
- [18] Baker J. W. (2011): Conditional Mean Spectrum: Tool for ground motion selection. *Journal of Structural Engineering*, 137(3), 322-331.
- [19] El Dakhkni W. W., Egaaly M., and Hamid A. (2003): Three Strut model for concrete masonry infilled steel frames. *Journal of Structural Engineering*, vol. 129, no. 2.
- [20] Öztürk M. S. (2005): Effects of masonry infill walls on the seismic performance of buildings. Msc. Thesis. *Middle East Technical University, Civil Engineering Department*.
- [21] Shing P. B., Stavridis A., Koutromanos I., Willam K., Blackard B., Kyriakides M. A. Billington S.L. , and Arnold S. (2009): Seismic performance of non-ductile RC frames with brick infill. *ATC & SEI Conference on Improving the Seismic Performance of Existing Buildings and Other Structures*.
- [22] Fenerci A. (2013): The effect of infill walls on the seismic performance of boundary columns in reinforced concrete frames. . Msc. Thesis. *Middle East Technical University, Civil Engineering Department*.